Electronic Supplementary Information

Novel electrochemical sensor for the determination of lidocaine based on surface-imprinting on porous three-dimensional film

Guangming Yang,[a,b] and Faqiong Zhao[a*]

[a] Key Laboratory of Analytical Chemistry for Biology and Medicine (Ministry of Education), College of Chemistry and Molecular Sciences, Wuhan University, Wuhan, Hubei, 400372, China, Fax: (+86)68752701, E-mail: fqzhao@whu.edu.cn

[b] Department of Resources and Environment, Baoshan University, Bao shan, Yunnan, 678000, China

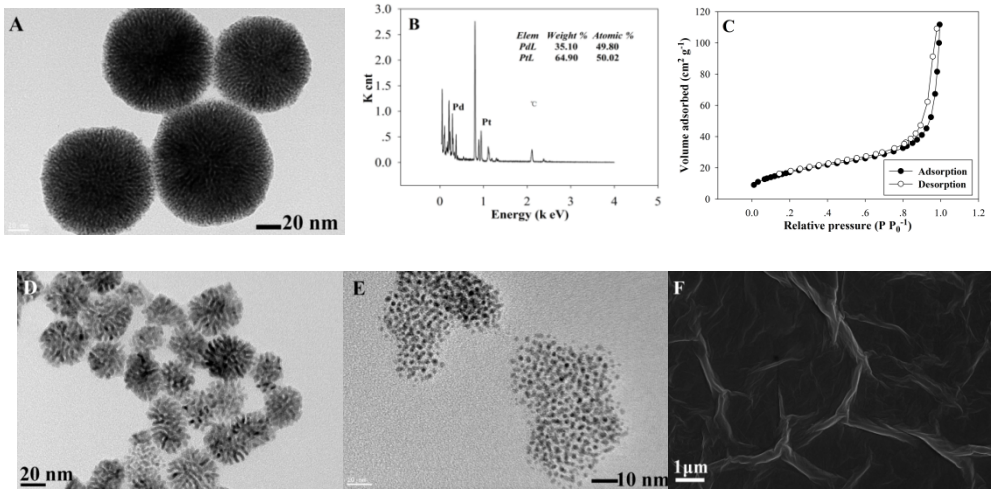

Fig. S1 The high-magnification TEM image of the dendritic Pd-Pt bimetallic nanoparticles (A), energy dispersive spectrum of the dendritic Pd-Pt bimetallic nanoparticles (B), The Brunauer-Emmett-Teller (BET) measurement of dendritic Pd-Pt bimetallic nanoparticles (C), high-magnification TEM image of dendritic Pd nanoparticles (D) and porous Pt nanonetworks (Pt NWs) (E), and the SEM image of carboxyl-graphene (COOH-r-GO) modified glassy carbon electorde (GCE) (F).

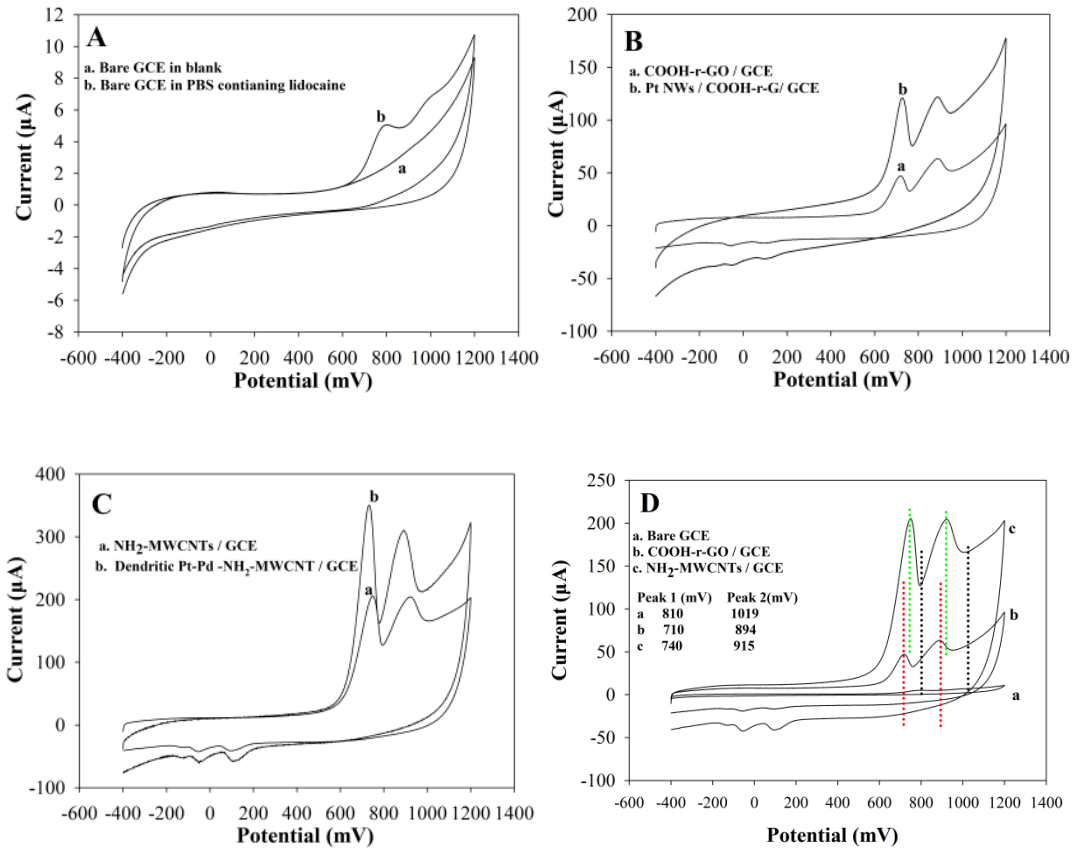

Fig. 2S **(A)** CVs of bare GCE in blank PBS (pH= 7.5) (a) and PBS + 1.0 × 10^{-5} mol L^{-1} lidocaine;

(B) CVs of COOH-r-GO / GCE and Pt NWs / COOH-r-GO / GCE in PBS containing 1.0 × 10^{-5} mol L^{-1} lidocaine;

(C) CVs of NH_2-MWCNTs / GCE and dendirtic Pt-Pd bimetallic nanoparticles-NH_2-MWCNTs / COOH-r-GO / GCE in PBS containing 1.0 × 10^{-5} mol L^{-1} lidocaine.

(D) CVs of bare GCE, COOH-r-GO / GCE and NH_2-MWCNTs / GCE in PBS containing 1.0 × 10^{-5} mol L^{-1} lidocaine.

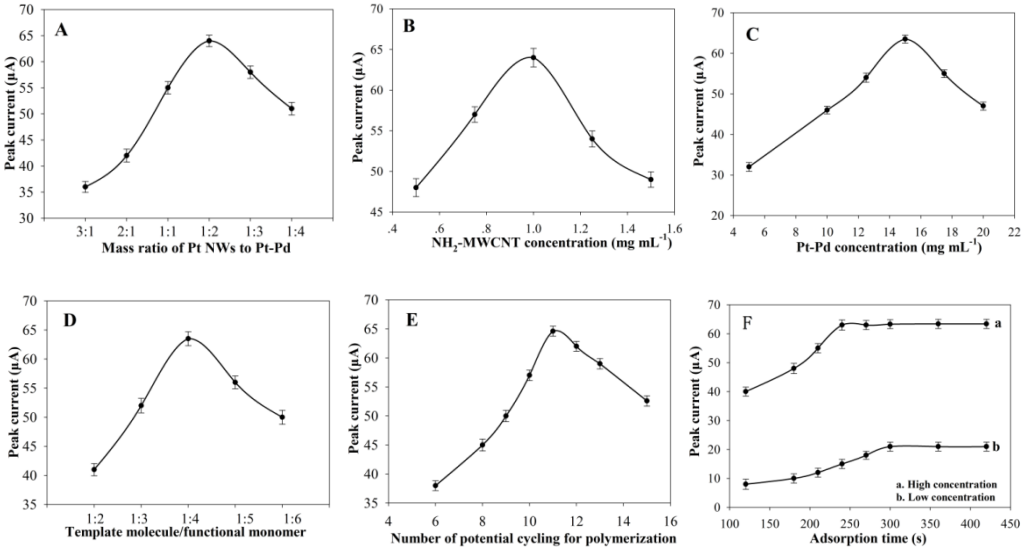

Fig. S3 Influence of different factors on the peak current of 1.0×10^{-6} mol L^{-1} lidocaine (A to F) in PBS (pH= 7.5). All error bars represent SD (n= 3). (A) Mass ratio of Pt NWs to dendritic Pt-Pd bimetallic NPs; (B) concentration of NH_2-MWCNT; (C) concentration of dendritic Pt-Pd bimetallic NPs; (D) ratio of template molecule to functional monomer; (E) electrochemical polymerization time; (F) adsorption time (a: 1.0×10^{-6} mol L^{-1}; b: 1.0×10^{-9} mol L^{-1} lidocaine).

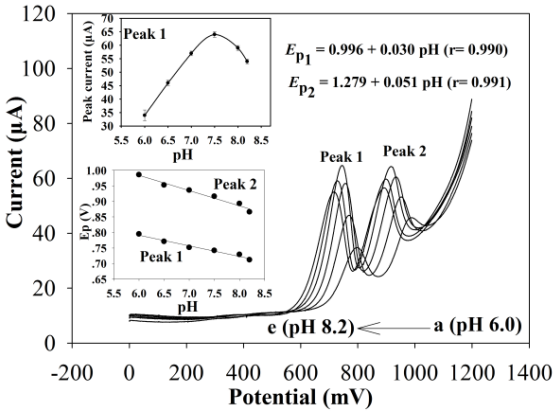

Fig. S4 DPVs of the MIP sensor in 1.0×10^{-6} mol L^{-1} lidocaine solutions with different pH. Inset: effects of solution pH on peak current and on peak potential of 1.0×10^{-6} mol L^{-1} lidocaine. Error bars represent SD (n=3). Other conditions as in Fig. S3.

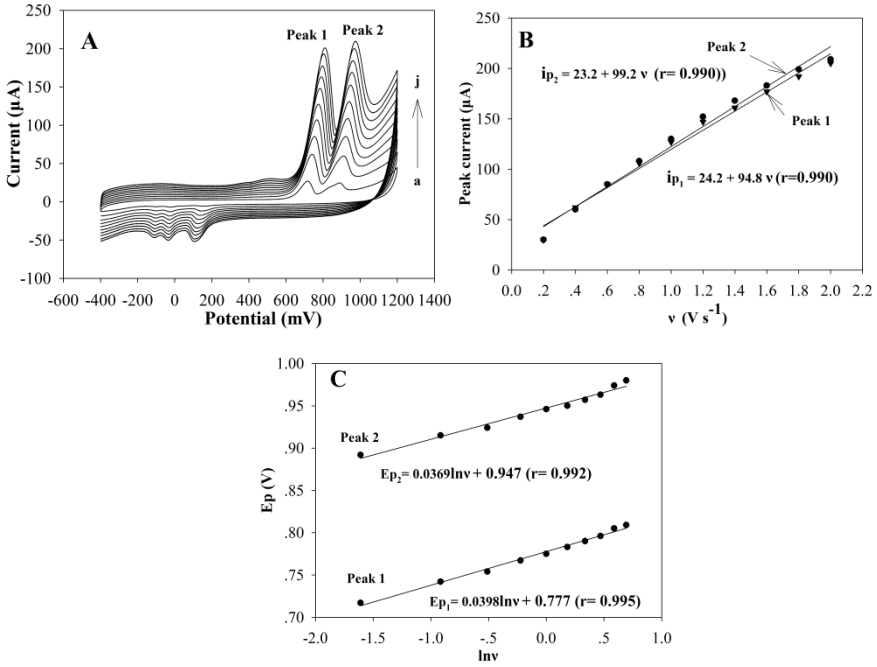

Fig. S5 (A) CVs of MIP sensors (I) at different scan rate in PBS (pH= 7.5) after binding lidocaine in 1.0×10^{-6} mol L^{-1} lidocaine. Scan rate (a to j): 20 to 200 mV s^{-1};

(B) Effect of scan rate on peak current after binding lidocaine in 1.0×10^{-6} mol L^{-1} lidocaine;

(C) Effect of scan rate on peak potential after binding lidocaine in 1.0×10^{-6} mol L^{-1} lidocaine. Other conditions as in Fig. S3.

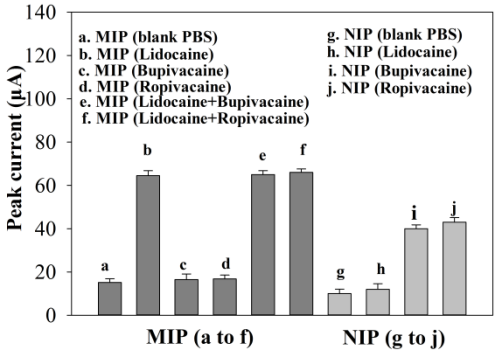

Fig. S6 Influence of similar compounds on the peak current of lidocaine in PBS (pH= 7.5) under optimal experimental conditions. Other conditions as in Fig. S3. Error bars represent SD (n=3). Solution composition for MIP sensor detection: (a) 0 mol L^{-1} lidocaine, (b) 1.0×10^{-6} mol L^{-1} lidocaine, (c) 2.0×10^{-5} mol L^{-1} ropivacaine, (d) 2.0×10^{-5} mol L^{-1} bupivacaine, (e) b + 2.0×10^{-5} mol L^{-1} ropivacaine and (f) b + 2.0×10^{-5} mol L^{-1} bupivacaine;

Solution composition for NIP sensor detection: (g) 0 mol L^{-1} lidocaine, (h) 1.0×10^{-6} mol L^{-1} lidocaine, (i) 2.0×10^{-5} mol L^{-1} ropivacaine and (j) 2.0×10^{-5} mol L^{-1} bupivacaine.